Published in final edited form as:
Dalton Trans. 2010 January 14; (2): 568–576. doi:10.1039/b914568k.

Toward the Development of Prochelators as Fluorescent Probes of Copper-Mediated Oxidative Stress†

Lynne M. Hyman[a], **Clifton J. Stephenson**[b], **Marina G. Dickens**[a], **Ken D. Shimizu**[b], and **Katherine J. Franz**[*,a]

[a]Department of Chemistry, Duke University, Durham, NC 27708-0346 USA

[b]Department of Chemistry and Biochemistry, University of South Carolina, USA

Abstract

A fluorescent sensor prochelator, FlamB (fluorescein hydrizido 2-imidophenylboronic ester), has been developed that selectively probes for copper under conditions of oxidative stress. High levels of hydrogen peroxide trigger release of a boronic ester masking group from the prochelator to unveil a metal chelator, FlamS (fluorescein hydrizido 2-imidophenol), that provides a modest fluorescence increase in response to Cu^{2+} but not other metal ions. X-ray crystal structures of FlamB, FlamS, and Cu-bound FlamS are all reported. The fluorescence turn-on results from opening of a fluorescein spirolactam ring upon Cu^{2+} binding to FlamS in aqueous solution. Oxidation of the aryl boronic ester of FlamB to the metal-binding phenol of FlamS proceeds in organic solvents. However, in aqueous solution a competing mechanism occurs due to hydrolytic instability of the masked prochelator. Hydrolysis of FlamB leads to formation of fluorescein hydrazide, which interacts with copper or H_2O_2 to produce fluorescein and a significant fluorescence increase.

Introduction

Copper is an essential cofactor for several enzymes; however, an imbalance in its cellular homeostasis can lead to uncontrolled redox chemistry and formation of toxic reactive oxygen species (ROS).[1] Copper, like iron, can participate in Fenton chemistry to form hydroxyl radicals (Eq. 1) and cause oxidative stress that leads to cell death. Metal-induced oxidative stress has been linked to several neurodegenerative diseases, including Alzheimer's and Parkinson's, wherein both copper and iron have been implicated.[2] Misregulation of cellular copper homeostasis is also linked to Menkes and Wilson diseases, familial amyotrophic lateral sclerosis, and prion diseases.[3–5] The implication that some disease states may be associated with exchange-labile pools of redox-active iron or copper has spurred the interest in developing fluorescent chemosensors to visualize their cellular distribution.

$$H_2O_2 + Cu^{+}OH^{\cdot} + OH^{-} + Cu^{2+} \qquad \text{(Eq. 1)}$$

Both reversible and irreversible fluorescence turn-on strategies for probing copper and iron have been reported and recently reviewed.[6] Developing fluorescence turn-on sensors for

†Electronic Supplementary Information (ESI) available: additional fluorescence and absorbance spectra, NMR spectra, and X-ray crystallographic details with full atom-numbering schemes. See DOI: 10.1039/b000000x/.

Fax: +1 919 660 1605; Tel: +1 919 660 1541; katherine.franz@duke.edu.

Cu^{2+} and $Fe^{2+/3+}$ is challenging due to inherent quenching from paramagnetic metal ions. However, several reports suggest that selective metal-dependent opening of a fluorescein or rhodamine spirolactam ring can be used to achieve an increase in fluorescence response for metal ions including Cr^{3+},[7, 8] Hg^{2+},[9–11] Co^{2+},[12] Pb^{2+},[13] Fe^{3+},[14, 15] and Cu^{2+}.[16–21] The aim of our current study is to utilize this strategy to create a fluorescence turn-on sensor that responds selectively to copper only under oxidative stress conditions.

Recently, our lab introduced BSIH (see Chart 1) as a prochelator to prevent metal-promoted oxidative damage in cells.[22–24] The design relies on selective conversion of a boronic ester masking group by H_2O_2 to the phenol of SIH, a high-affinity metal chelator. In the masked form, the prochelator does not interact with metal ions, whereas activation with H_2O_2 releases the unmasked chelator that coordinates metal ions and prevents both iron and copper from catalyzing $OH^{\bullet}$ production. In principle, this strategy allows sequestration and inactivation of detrimental metal ions at the site of oxidative stress without disrupting healthy metal homeostasis. Equipping a BSIH-like prochelator with a fluorescent tag would allow visualization of this H_2O_2-dependent metal sequestration. It would be particularly desirable to have probes that can differentiate iron- vs. copper-mediated oxidative stress in order to decipher the individual roles of these metal ions. An anthracene-appended boronic acid prochelator was recently shown to give a fluorescence quenching response in the presence of Fe^{3+}.[25] Here we introduce FlamB (see Chart 1) as a fluorescein-appended prochelator that gives a selective, albeit modest, fluorescence turn-on response for Cu^{2+} following reaction with H_2O_2. While it is desirable to have probes that operate under aqueous conditions at physiological pH, our first-generation probe discussed herein is not stable under these conditions, but provides a guidepost for future designs.

Results

Synthesis and structure of FlamB and FlamS

In order to create a fluorescent prochelator, we sought to embed a fluorophore directly within the backbone of our parent BSIH prochelator architecture. The isonicotinic acid hydrazide used to synthesize BSIH and SIH was therefore replaced by fluorescein hydrazide (FH) and reacted with either 2-formylphenyl boronic ester or salicylaldehyde to give FlamB and FlamS, respectively. The name FlamB derives from ***f***luorescein–***la***cta***m***–***b***oronate. Salicylaldehyde fluorescein hydrazone was recently published as a colorimetric logic chemosensor[26] and herein referred to as FlamS, where the S derives from salicylaldehyde. The condensation reactions to synthesize FlamB and FlamS were carried out in refluxing ethanol and the products were isolated by recrystallization from toluene or acetonitrile, respectively, in greater than 80 % yields.

The chemical structure of FlamB is similar to a recently published boronic acid version, where the boronic acid functionality was reported to interact directly with Cu^{2+} to effect a fluorescence response.[27] In contrast to that design, the pinacol ester of FlamB was installed to prevent metal interactions of the prochelator probe prior to its activation by H_2O_2 and conversion to FlamS. Once converted to FlamS, metal chelation through the phenolate O, imine N, and carbonyl O would initiate opening of the spirolactam ring with a concomitant increase in fluorescence emission.[21]

Both compounds are isolated in their non-fluorescent forms where the spirolactam ring is closed, as verified by the X-ray crystal structures shown in Fig. 1.‡ Similarities are found in the X-ray crystal structures of FlamB and FlamS when compared to BSIH and SIH. As with BSIH, the boron atom is *anti* to the imine N2 atom and the configuration around the C21=N2 bond is *E*. Similar to SIH, FlamS retains the *E* conformation, but the phenolic OH is *syn* to the imine nitrogen. However, unlike SIH, FlamS is not pre-arranged for metal

chelation, as the carbonyl and phenolate O atoms are on opposite faces. In both FlamB and FlamS structures, the xanthene ring is perpendicular to the ligand backbone, with a slight bend in the xanthene unit. In FlamS the 3-ring unit bends away from the phenol, whereas in FlamB the concave bend cradles the boronic ester.

Absorbance and fluorescence response of FlamS with Cu^{2+}

FlamS is insoluble in purely aqueous solution but dissolves in organic solvents such as methanol, DMSO, and acetonitrile. Due to these solubility limitations, solutions of FlamS were first prepared in DMSO and then diluted in buffer. When dissolved in 10 mM HEPES (4-(2-hydroxyethyl)-1-piperazineethanesulfonic acid) buffer at pH 7.4 containing 40% (v/v) DMSO, FlamS forms a colorless solution. An orange/yellow color appears upon addition of Cu^{2+} salts and an intense band is seen at 500 nm in the absorbance spectrum. Fig. 2a shows the absorbance spectra as a function of added Cu^{2+}. No additional spectral changes are observed when more than 1 equivalent of Cu^{2+} is added, suggesting the formation of a 1:1 coordination complex. Analysis of 1:1 FlamS and $CuSO_4$ solutions in MeOH by electrospray ionization mass spectrometry gives a molecular ion peak of 512.0 m/z, which is consistent with formation of $[Cu(FlamS)]^+$.

The appearance of the 500 nm absorption band indicates that the spirolactam ring is open and predicts that a corresponding fluorescence emission should turn on when solutions of Cu^{2+} and FlamS are excited near 500 nm. Such behavior is consist with the well discussed off/on fluorescence switch utilized in several rhodamine and fluorescein-based metal cation probes where the spirolactam ring is closed and colorless in solution until a metal ion binds, opening the ring and producing a fluorescent signal.[19] The emission spectra shown in Fig. 2b reveal only a modest doubling in emission intensity. The fluorescence enhancement due to spirolactam ring opening therefore appears to be counterbalanced by quenching due to Cu^{2+}, thereby giving only a moderate overall change in emission intensity. The quantum yield measurements bear this out, with a low value for the Cu-bound form in mixed aqueous solution (Φ= 0.004), which indicates that the fluorescence is essentially quenched. Even though the emission intensity is lower in the absence of Cu^{2+}, the quantum yield of FlamS alone is actually higher (Φ = 0.06). This apparent discrepancy arises because quantum yield calculations (see Experimental Section) take into account the integrated fluorescence emission as well as the absorbance at the excitation wavelength, which is negligible for FlamS without Cu^{2+}, but has a significant contribution for the Cu^{2+} complex.

The binding of Cu^{2+} to FlamS is reversible, as shown by a competition experiment where an equivalent of ethylenediaminetetraacetic acid (EDTA), a hexadentate metal chelator, added to a buffered solution of $[Cu(FlamS)]^+$ shows complete restoration of the absorbance spectrum of FlamS. The corresponding fluorescence spectra show that addition of EDTA causes the expected decrease in emission, although the level does not return to the original spectrum of FlamS (see ESI). The origin of this residual fluorescence intensity is not clear, but may indicate a small fraction of the Cu-bound form still present or a fluorescent decomposition product. In either case, its concentration is too low to provide any signal in the absorbance spectrum.

---

‡Crystallographic data (CCDC reference numbers 740843 – 740845): **FlamS**, $C_{31}H_{18}D_6N_4O_5$, M = 538.58, monoclinic, *a* = 14.8323(6) Å, b = 9.7901(4) Å, c = 18.5178(7) Å, β = 99.245(1)°, V = 2654.04(18) Å3, T = 150 (2) K, space group $P2_1/n$, Z=4, 43700 reflections measured, 5427 independent (R_{int} = 0.046). The final R indices [I>2sigma(I)] were R1 = 0.043, wR2 = 0.106. **FlamB**, $C_{34}H_{35}BN_2O_8$, M = 610.45, triclinic, a = 9.6200(3) Å, b = 12.0315(4) Å, c = 14.4614(5) Å, α = 100.699 (2)°, β = 107.549(2)°, γ = 99.854(2)°, V = 1521.39(9) Å3, T = 296(2) K, space group P-1, Z = 2, 23306 reflections measured, 5114 independent (R_{int} = 0.042). The final R indices [I>2sigma(I)] were R1 = 0.0598, wR2 = 0.1703. **CuFlamS**, $C_{27}H_{17.5}ClCuN_2NaO_{5.5}$, M = 565.67, monoclinic, a = 17.948(3) Å, b = 36.076(6) Å, c = 17.331(2) Å, β = 120.278(6)°, V = 9691(3) Å3, T = 100(2) K, space group C2/c, Z = 16, 34579 reflections measured, 4691 observed (R_{int} = 0.067). The final R indices [I>2sigma(I)] were R1 = 0.0736, wR2 = 0.1942. For crystallographic data in CIF format see DOI: 10.1039/b000000x/.

Unlike the absorption spectra seen in aqueous solution, solutions of $[Cu(FlamS)]^+$ in organic solvent do not show a feature at 500 nm. Fig. 3 compares the spectra of crystalline $[Cu(FlamS)]^+$ dissolved in methanol or a methanol/water mixture. A copper complex clearly forms in organic solvent, as indicated by the yellow color of the solution and the band at 417 nm; however, the absence of signal at 500 nm indicates that the spirolactam ring is closed under these conditions. As predicted based on the absorbance spectra, no change in fluorescence is observed for FlamS upon addition of copper in organic solvent. Introduction of water to this solution leads to electron redistribution and subsequent proton transfer to produce the ring-open form, which restores the 500 nm absorbance peak and corresponding fluorescence enhancement.

Structure of Cu-bound FlamS

Reactions in methanol of FlamS with one equivalent of $CuCl_2$ as the copper source and NaOH as a base yielded brown, ellipsoid-shaped crystals grown by slow evaporation from a methanol/ethanol mixed solvent. The X-ray crystal structure in Fig. 4 shows that the complex crystallizes in a tetranuclear arrangement composed of a dimer of $[Cu_2Cl(FlamS)_2]Cl$ units. The structure validates the overall 1:1 ligand:metal ratio. Each square pyramidal Cu(II) center is coordinated by a carbonyl O, imine N, and phenolate O of one FlamS molecule, with a phenolate O from an adjacent Cu–FlamS unit acting as a bridging ligand between two Cu centers to complete their square pyramid bases. A Cl^- ligand occupies the apical position, and bridges to a Cu center of the second dimer to form the tetranuclear structure. Two outer-sphere Cl^- ions are present to balance the charge. As predicted from the solution experiments in organic solvent, the structure of the complex isolated from methanol/ethanol has the spirolactam ring in the closed form.

Metal specificity of FlamS

The sensitivity of the fluorescence turn-on response to other biologically relevant metal cations was examined. Aqueous solutions of Fe^{3+}, Fe^{2+}, Ni^{2+}, Zn^{2+}, Mn^{2+}, Cd^{2+}, Hg^{2+}, Pb^{2+}, Co^{2+}, Ag^+, Ca^{2+} and Mg^{2+} were titrated into solutions of FlamS and changes to the emission and absorbance spectra were monitored. Up to 2 equivalents of the transition metals were added, while Ca^{2+} and Mg^{2+} were titrated into FlamS solutions in concentrations up to 5 mM. Following these titrations, one equivalent of Cu^{2+} was added to the FlamS-metal solutions to ensure restoration of the turn-on emission response.

Fig. 5 shows the data plotted as a bar graph with emission intensities normalized to that of the Cu^{2+}-bound FlamS. None of the other metal ions tested gives a positive fluorescence response between 500–600 nm when excited at 500 nm. Likewise, no changes are seen in the absorbance spectrum of FlamS upon addition of these metal ions (ESI). Fluorescence emission at 520 nm (Fig. 5) and the absorbance band at 500 nm are restored once Cu^{2+} is added back into the system for most of the metals. In the unique cases of Hg^{2+} and Fe^{2+}, full restoration of the emission signal is not seen. In the case of Hg^{2+}, this could be due to a quenching effect of the metal in solution, as full recovery of the spirolactam's absorbance band at 500 nm is seen once Cu2+ is added to the system. However, the band at 500 nm is not fully restored when Cu^{2+} is added to a FlamS-Fe^{2+} solution, possibly indicating a competition for binding which lowers the copper response. The results of the metal specificity studies verify that opening of the spirolactam ring is sensitive only to Cu^{2+}.

Spectral response of FlamB

To confirm that the boronic ester mask prevents the prochelator from interactions with copper, solutions of FlamB were titrated with Cu^{2+} and monitored spectrophotometrically. As predicted, no new spectral features appear in the UV-vis spectrum of FlamB in DMSO when titrated with Cu^{2+} (see ESI). Likewise, the fluorescence spectrum of FlamB in organic

solvent, which is nearly completely quenched, does not change upon addition of Cu^{2+} (ESI). These results are consistent with the design that the prochelator has little to no affinity for copper in its masked form.

While the lack of metal binding of FlamB is a promising feature for the prochelator probe, FlamB itself is not stable in aqueous solution. Fig. 6 shows the absorbance spectra of FlamB dissolved in 60/40 HEPES buffer/DMSO over time. The decrease in the absorbance peak at 325 nm demonstrates the instability of FlamB in buffered solution at pH 7.4, with a half-life of 12 min. The hydrolysis of FlamB into its hydrazide and aldehyde components is nearly complete after 1.5 h in the HEPES buffer/DMSO mixed solvent, as verified by the identification of the hydrolysis product fluorescein hydrazide (FH) by the LC-MS analysis shown in the middle panel of Fig. 7. In contrast, FlamS remains intact under the same conditions, as seen in the bottom panel of Fig. 7. Analysis of the chromatography trace shows that after 1.5 h, less than 2% of FH is released from solutions of FlamS.

We had initially observed that an aqueous solution of FlamB titrated with Cu^{2+} yields a strong increase in fluorescence emission. However, this fluorescence increase is *not* a result of FlamB itself, but rather of the hydrolyzed product FH. As has been shown by others and confirmed here (see ESI), FH reacts selectively with Cu^{2+} to give a greater than 16-fold emission increase.[18, 19] Scheme 1 shows the proposed mechanism, where Cu^{2+} binding to FH in aqueous solution opens the spirolactam ring and cleaves the amide bond to release highly fluorescent fluorescein. The interaction between FH and Cu^{2+} is irreversible, as verified by the lack of competition with EDTA (ESI). This result further supports the conclusion that FlamB hydrolyzes rapidly in aqueous solution.

Conversion of FlamB to FlamS with H_2O_2

Because of the instability of FlamB in aqueous solution, the oxidative conversion of FlamB to FlamS by H_2O_2 was monitored in organic solvent. Fig. 8 shows the UV-vis traces arising from the reaction of FlamB with excess H_2O_2 in DMSO. The clean conversion is characterized by a shift in the absorbance peak at 325 nm to 334 nm. The absorbance data fit a pseudo first-order process to give $k_{obs} = 2.1 \times 10^{-5}\ s^{-1}$. The products from the reaction were confirmed to be FlamS by NMR analysis (with characteristic peaks at 6.47, 6.64, 6.78, and 7.22 ppm in *d*-DMSO) and a product consistent with released boronate pinacol ester, where the signal for the pinacol methyl protons (1.15 ppm) are shifted from that seen in either FlamB (1.25 ppm) or the free pinacol diol (1.07 ppm).

Further confirmation that the product of FlamB oxidation by H_2O_2 in organic solvent is FlamS is the observation that addition of Cu^{2+} to the reaction solution results in formation of $[Cu(FlamS)]^+$, as shown in Fig. 9. Because the experiment is done in organic solvent, the copper complex is in the ring-closed form that lacks the absorption band at 500 nm and is non-fluorescent. Addition of water to the DMSO solution converts it to the ring-open form with a 2-fold fluorescence-enhanced spectrum.

Discussion

In order to design a fluorescence sensor that could distinguish toxic copper that is participating in damaging redox activity from healthy cellular copper, we sought a molecular scaffold that would lack fluorescence and metal-binding properties until conditions of metal-catalyzed oxidative stress were encountered. Scheme 1A shows the mechanism of how we envisioned the prochelator probe FlamB to operate to give a fluorescence turn-on response in the presence of both H_2O_2 and Cu^{2+}. Fusing an aryl boronic ester to fluorescein through an aroyl hydrazone linkage creates the prochelator FlamB, where the closed spirolactam ring prevents fluorescence and the boronic ester prevents metal coordination. The aryl boronic

ester also provides the oxidative stress trigger, since its conversion to the phenol of FlamS requires H_2O_2, a key ingredient in the Fenton reaction that leads to metal-catalyzed oxidative stress (Eq. 1). Once unmasked, FlamS is available for metal binding. Work by others[21, 26] and reproduced here shows the FlamS chelator to be specific for Cu^{2+}, even in the presence of other metal ions like Fe^{3+}, Fe^{2+}, Ni^{2+}, Zn^{2+}, Mn^{2+}, Cd^{2+}, Hg^{2+}, Pb^{2+}, Co^{2+}, Ag^{+}, Ca^{2+} and Mg^{2+}.

We have shown here that each of the steps indicated in Scheme 1 pathway (A) is indeed feasible, but unfortunately not under the same solution conditions. In particular, the hydrazone linkage of FlamB is sensitive to hydrolysis in aqueous solution and decomposes into its hydrazide and aldehyde components within minutes. Aroylhydrazones are known to be unstable under certain solution conditions, especially in cell culture media and plasma, although they are generally stable in simple buffered solutions.[28–30] In our previous studies with SIH and BSIH, we found that both compounds are stable in phosphate buffer at pH 7.4, but SIH decomposes within hours in cell culture media at 37 °C, while BSIH remains intact over 24 h in the same conditions.24 The current result that FlamB is unstable in aqueous solution is therefore in stark contrast to the stability of its non-fluorophore parent compound BSIH.

The consequence of the hydrolytic decomposition shown in Scheme 1 pathway (B) is the loss of H_2O_2-dependent chelator activation that is part of the intended design in pathway (A). The fluorescein hydrazide (FH) product is known to interact readily with Cu^{2+} as shown in pathway (B) to yield fluorescein as the final product.[18, 19] FH-to-fluorescein conversion also occurs via reaction with H_2O_2, as recently demonstrated.[31] Fluorescein has an intense fluorescence emission with a high quantum yield, so even a small amount of released fluorescein would overwhelm the weak emission provided by $[Cu(FlamS)]^{+}$.

In organic solvents, the spirolactam ring of the Cu^{2+}-bound form remains closed and the complex is non-fluorescent. Addition of water leads to rearrangement of the complex and opening of the ring, thus activating fluorescence. In our hands, we see a modest 2-fold fluorescence enhancement caused by Cu^{2+} binding to FlamS. The fact that the strong band at 500 nm in the absorbance spectrum does not correlate with a correspondingly large increase in the fluorescence emission spectrum suggests that while the spirolactam ring is indeed in the open amide form, the presence of Cu^{2+} quenches emission to leave only residual intensity with a quantum yield of 0.004. In contrast to our results, a rhodamine analog of FlamS was shown to give a more significant 9-fold enhancement in buffered aqueous solution at pH 7.0, although a quantum yield was not reported.[21]

A compound related to FlamB containing a rhodamine instead of fluorescein core and a boronic acid in place of the pinacol boronic ester has also been reported.[27] The $B(OH)_2$ unit is proposed to bind Cu^{2+} directly to facilitate spirolactam ring opening to give an 8-fold fluorescence enhancement and an increase in quantum yield from 0.07 in the absence of Cu^{2+} to 0.45 in the presence of 100-fold excess Cu^{2+}.[27] The quantum yield of the metal-free form is consistent with our results for FlamS and FlamB, but the significant increase in quantum yield for the copper complex is distinctive. The structure of the Cu^{2+} complex of the boronic acid rhodamine probe is not known, but given the significant quenching effect that Cu^{2+} has on the ring-open amide form of FlamS, it would be interesting to understand how the boronic acid version achieves the much larger fluorescence enhancement. No indications of hydrolytic decomposition of the boronic acid rhodamine hydrazone probe were reported, although it should be noted that samples of metal and probe were prepared in acetonitrile prior to dilution into buffer for fluorescence measurements. Hydrolysis of the probe would not be noted in this case, as pre-assembly of the Cu^{2+} complex stabilizes the compound against hydrolysis.

Conclusion

By masking a copper sensor with a boronic ester, we have made progress in developing a strategy for probing metal-mediated oxidative stress by fluorescence. Our design utilizes hydrogen peroxide to unmask a metal chelator, which upon copper binding produces a modest fluorescence turn-on response. Metal-dependent opening of a fluorescein or rhodamine spirolactam ring has become a popular strategy for achieving metal-selective fluorescence turn-on responses. Our results, however, indicate that such a boost in fluorescence is actually greatly minimized, at least in the case of Cu^{2+}, such that the overall gain in intensity is unlikely to be bright enough for cellular applications.

Our results further emphasize the need to carefully monitor for alternative pathways of fluorescence increase. Hydrolysis of FlamB results in formation of fluorescein hydrazide, which produces a greater than 16-fold increase in fluorescence emission due to formation of fluorescein upon interaction with Cu^{2+} or H_2O_2. The instability of FlamB therefore provides an alternative, unintended pathway to fluorescence that derives from degradation of the original probe rather than a direct interaction of the probe with its target metal ion. Even if the compound were stable in simple aqueous buffers, exposure to cell culture media is known to have a dramatic influence on the stability of hydrazone-containing compounds. Our results highlight the importance of determining the stability of hydrazone compounds in appropriate solution conditions, since the mechanism of fluorescence change may be unintended. Despite this alternate pathway for FlamB, we verified that oxidation by H_2O_2 followed by subsequent copper binding occurs in organic solvents. Our results provide a template for future probe designs with improved properties. With this in mind, we are currently redesigning probes with less hydrolysis-prone linkages.

Experimental

Materials and instrumentation

All chemicals were purchased from Fisher Scientific or Sigma-Aldrich and used without further purification. All solvents were reagent grade and all aqueous solutions were prepared from nanopure water. FlamB, FlamS, and FH stock solutions (2 mM) were prepared daily in DMSO. Liquid chromatography-electrospray mass spectrometry (LC-MS) was performed using an Agilent 1100 Series apparatus with an LC/MSD trap and a Daly conversion dynode detector. A Varian Polaris C18 (150 × 1.0 mm) column was used and peaks were detected by UV absorption at 254 nm. A linear gradient from 10% A in B to 60% A in B was run at 40 μL/min from 2–17 min with a total run time of 22 min, where A is MeCN/2% 10 mM ammonium acetate buffer and B is 10 mM ammonium acetate buffer/2% MeCN. ^{1}H and ^{13}C NMR spectra were recorded on a Varian 300 or 400 mHz NMR spectrometer; δ values are in ppm and *J* values are in Hz. Flash chromatography was done using Silicycle Silia-P flash silica gel and TLC was done using silica gel 60 F_{254} precoated plates purchased from EDM Chemicals Inc. UV-vis spectra were recorded on a Cary 50 UV-vis spectrophotometer. Emission spectra were recorded on a Jobin-Yvon-Horiba Fluorolog 3 fluorimeter in a 1-cm pathlength quartz cell. Excitation and emission slit widths were 5 nm and emission spectra were collected from 500–600 nm after excitation at 495 nm. Elemental analysis was performed by Columbia Analytical Services, Tucson, AZ.

Synthesis

Preparation of fluorescein hydrazine (FH)—Fluorescein (0.168 g, 0.5 mmol) was dissolved in 200 mL ethanol. Hydrazine hydrate (65% in H_2O; 0.146 mL, 3.0 mmol) was added dropwise and the stirred reaction mixture was heated at reflux for 4 h. The solvent was removed under vacuum and the product was recrystallized from MeCN to give a yellow

solid (0.138 g, 80% yield). ^{1}H NMR spectra of the product matched the previously reported spectra[18] and was also verified by x-ray crystallography.[31] ^{1}H NMR (300 MHz DMSO-d_6) δ 7.76 (dd, *J* 5.7 and 3, 1 H), 7.47 (dd, *J* 3.75 and 3.75, 2 H), 6.96 (dd, *J* 5.25 and 3.75, 1 H), 6.57 (d, *J* 2.7, 2 H), 6.36–6.45 (m, 4 H), 4.36 (s, 2 H). ESI-MS: *m/z* 347.1 $[M+H]^+$, calcd 346.1 for M = $C_{20}H_{14}N_2O_4$; UV-vis λ_{max}(DMSO)/nm 277 (ε/dm^3 mol^{-1} cm^{-1} 6887).

Preparation of fluorescein hydrizido 2-imidophenol (FlamS)—FH (0.300 g, 0.867 mmol) was dissolved in 15 mL of absolute ethanol. Salicylic benzaldehyde (0.361 mL, 3.39 mmol) was added, and the stirred reaction mixture was heated under reflux conditions for 20 h. The solvent was removed under vacuum, and the product was recrystallized from acetonitrile to yield a yellow solid (0.322 g, 82.6%). ^{1}H NMR (300 MHz, CD_3CN) δ 10.57 (s, 2H), 9.27 (s, 1H), 7.97 (dd, *J* 5.1 and 1.8, 1H), 7.62–7.66 (m, 2H), 7.21–7.30 (m, 2H), 7.17 (dd, *J* 5.7 and 1.8, 1H), 6.88 (dd, *J* 7.6 and 7.6, 1H), 6.72 (d, *J* 2.7, 2H), 6.64 (d, *J* 8.7, 2H), 6.53 (dd, *J* 8.7 and 2.4, 2H). ^{13}C NMR (100 MHz, CD_3CN) δ 166.289, 163.46, 158.69, 157.16, 152.14, 150.44, 150.22, 134.142, 131.85, 129.04, 128.75, 128.12, 123.86, 123.25, 119.43, 118.92, 116.36, 112.528, 109.45, 102.51, 65.21. HRMS (EI): calcd for $C_{27}H_{18}N_2O_5$ 450.1207; found 450.1216. UV-vis (40% DMSO in 10 mM HEPES/100 mM NaCl, pH 7.4), λ_{max}/nm 280 (ε/dm^3 mol^{-1} cm^{-1} 11 718), 340 (13 907).

Preparation of fluorescein hydrizido 2-imidophenylboronic ester (FlamB)—To a solution of FH (0.200 g, 0.578 mmol) in absolute ethanol (15 mL) was added 2-formylphenylboronic acid pinacol ester (0.391 mL, 1.77 mmol). The reaction mixture was stirred for 10 min at rt at which time TLC showed that the FH starting material had fully reacted. The solvent was removed under vacuum, and the product was recrystallized from toluene as a yellow solid. (0.288 g, 89 %). ^{1}H NMR (400 MHz, CD_3CN) δ 9.72 (s, 1H), 7.93 (d, *J* 6.8, 1H), 7.76 (d, *J* 7.9, 1H), 7.71 (d, *J* 7.4, 1H) 7.57–7.62 (m, 2H), 7.42 (dd, *J* 7.0 and *J* 7.0, 1H), 7.35 (dd, *J* 7.2 and *J* 7.2, 1H), 7.29 (s, 2H), 7.15 (d, *J* 6.4, 1H) 6.73 (d, *J* 2.4, 2H), 6.64 (d, *J* 8.4, 2H), 6.50 (dd, *J* 8.8 and *J* 2.4, 2H), 1.32 (s, 12H). ^{13}C NMR (100 MHz, CD_3CN) δ 165.40, 159.15, 153.96, 151.56, 151.56, 141.40, 136.75, 134.82, 132.03, 130.28, 130.18, 129.01, 125.25, 124.54, 124.35, 112.98, 112.87, 104.05, 85.21, 25.12. HRMS (EI): Calcd for $C_{33}H_{29}BN_2O_6$ 560.2125; found 560.2138. UV-vis λ_{max}(DMSO)/nm 325 (ε/dm^3 mol^{-1} cm^{-1} 16 417).

Preparation of $[Cu_2Cl(FlamS)_2]_2Cl_2$—A 50 mM aqueous solution of NaOH (1.334 mL) was added dropwise to a refluxing solution of FlamS (0.030 g, 0.067 mmol) and $CuCl_2$•$2H_2O$ (0.0114 g, 0.067 mmol) in 20 mL EtOH. After refluxing for 1 h, the solvent was removed and the residue was taken up in acetone and filtered. The acetone was removed and the residue was taken up in 50% MeOH and 50% EtOH. Slow evaporation gave amber, ellipsoid-shaped crystals in 30% yield. ESI-MS: *m/z* 512.0 $[M]^+$ and 530.0 $[M+H_2O]^+$, calcd 512.04 for M = $C_{27}H_{17}CuN_2O_5$; UV-vis λ_{max}(40% DMSO in 10 mM HEPES/100 mM NaCl, pH 7.4)/nm 503 (ε/dm^3 mol^{-1} cm^{-1} 27 622); Anal. Calcd. for $C_{27}H_{17}ClCuN_2O_5$·NaOH: C, 55.11; H, 3.08; N, 4.76; found C, 54.84; H, 3.21; N, 4.42.

Kinetics—The rate of oxidation of FlamB to FlamS was investigated under pseudo first-order conditions of excess H_2O_2. In a typical study, 3 mL of a 40 μM solution of FlamB in DMSO were loaded into a quartz cuvette. H_2O_2 (50 % wt solution in H_2O) was added to a final concentration of 3 mM. The reaction was monitored up to 2 h and spectra were collected at 2 min time intervals. The negative slope of the linear fit of ln(Abs) at λ_{max} of FlamB (325 nm) vs. time plot provided the observed rate constant (k_{obs}).

Quantum yield—Stock solutions were prepared of 1 mM FlamS in DMSO and 1 mM $[Cu(Glycine)_2]$ in HEPES (4-(2-hydroxyethyl)-1-piperazineethanesulfonic acid) buffer (10

mM, pH = 7.4) containing 40% (v/v) DMSO. Dilutions of $[Cu(FlamS)]^+$ at 1, 2, 3, 4, and 5 μM were prepared in the HEPES/DMSO mixed solvent using 10 equivalents of $[Cu(Glycine)_2]$. Absorbance and emission measurements were taken in triplicate. Excitation was performed at 495 nm and collected emission was normalized to the HEPES/DMSO mixed solvent blank and then integrated from 500 to 600 nm. A plot of the integrated fluorescence intensity vs. the absorbance at 495 nm for each concentration was prepared and the positive slope of the linear fit was calculated. The data were compared to a fluorescein standard in 1 M NaOH using the following equation (Eq. 2), where ϕ_R is the quantum yield of the standard (0.95), Grad is the slope of the absorbance vs. emission line found for $[CuFlamS]^+$, $Grad_R$ is the slope found for the fluorescein standard, η is the refractive index of the $[CuFlamS]^+$ solution (1.3938) and η_R is the refractive index of the fluorescein solution (1.33):

$$\phi=\phi_R(\mathrm{Grad}/\mathrm{Grad}_R)(\eta^2/\eta_R{}^2) \quad \text{(Eq. 2)}$$

Acknowledgments

KJF thanks the Sloan Foundation, the Camille and Henry Dreyfus Foundation, the National Institutes of Health (grant GM084176) and Duke University for support, MGD acknowledges a C. R. Hauser fellowship, and KDS acknowledges NSF grant CHE 0616442 for support.

References

1. Kim B-E, Nevitt T, Thiele DJ. Nat. Chem. Biol 2008;4:176–185. [PubMed: 18277979]
2. Barnham KJ, Masters CL, Bush AI. Nat. Rev. Drug Disc 2004;3:205–214.
3. Brown DR, Kozlowski H. Dalton Trans 2004:1907–1917. [PubMed: 15252577]
4. Gaggelli E, Kozlowski H, Valensin D, Valensin G. Chem. Rev 2006;106:1995–2044. [PubMed: 16771441]
5. Madsen E, Gitlin JD. Annu. Rev. Neurosci 2007;30:317–337. [PubMed: 17367269]
6. Que EL, Domaille DW, Chang CJ. Chem. Rev 2008;108:1517–1549. [PubMed: 18426241]
7. Zhou Z, Yu M, Yang H, Huang K, Li F, Yi T, Huang C. Chem. Commun 2008:3387–3389.
8. Mao J, Wang L, Dou W, Tang X, Yan Y, Liu W. Org. Lett 2007;9:4567–4570. [PubMed: 17900133]
9. Wu D, Huang W, Duan C, Lin Z, Meng Q. Inorg. Chem 2007;46:1538–1540. [PubMed: 17266305]
10. Yang Y-K, Yook K-J, Tae J. J. Am. Chem. Soc 2005;127:16760–16761. [PubMed: 16316202]
11. Lee MH, Wu J-S, Lee JW, Jung JH, Kim JS. Org. Lett 2007;9:2501–2504. [PubMed: 17530763]
12. Yang X-F, Wu D-B, Li H. Microchim. Acta 2005;149:123–129.
13. Zhang X, Shiraishi Y, Hirai T. Tetrahedron Lett 2007;48:5455–5459.
14. Xiang Y, Tong A. Org. Lett 2006;8:1549–1552. [PubMed: 16597107]
15. Zhang M, Gao Y, Li M, Yu M, Li F, Li L, Zhu M, Zhang J, Yi T, Huang C. Tetrahedron Lett 2007;48:3709–3712.
16. Zhang X, Shiraishi Y, Hirai T. Org. Lett 2007;9:5039–5042. [PubMed: 17975919]
17. Yu M, Shi M, Chen Z, Li F, Li X, Gao Y, Xu J, Yang H, Zhou Z, Yi T, Huang C. Chem. Eur. J 2008;14:6892–6900.
18. Chen X, Ma H. Anal. Chim. Acta 2006;575:217–222. [PubMed: 17723594]
19. Dujols V, Ford F, Czarnik AW. J. Am. Chem. Soc 1997;119:7386–7387.
20. Xiang Y, Tong A. Luminescence 2007;23:28–31. [PubMed: 18175362]
21. Xiang Y, Tong A, Jin P, Ju Y. Org. Lett 2006;8:2863–2866. [PubMed: 16774276]
22. Charkoudian LK, Pham DM, Franz KJ. J. Am. Chem. Soc 2006;128:12424–12425. [PubMed: 16984186]

23. Charkoudian LK, Pham DM, Kwon AM, Vangeloff AD, Franz KJ. Dalton Trans 2007;43:4873–5092.
24. Charkoudian LK, Dentchev T, Lukinova N, Wolkow N, Dunaif JL, Franz KJ. J. Inorg. Biochem 2008;102:2130–2135. [PubMed: 18835041]
25. Wei Y, Guo M. Chem. Commun 2009:1413–1415.
26. Chen X, Li Z, Xiang Y, Tong A. Tetrahedron Lett 2008;49:4697–4700.
27. Swamy KMK, Ko S, Kwon SK, Lee HN, Mao C, Kim J, Lee K, Kim J, Shin I, Yoon J. Chem. Commun 2008;45:5915–5917.
28. Buss JL, Ponka P. Biochim. Biophys. Acta 2003;1619:177–186. [PubMed: 12527114]
29. Kovarikova P, Klimes J, Sterba M, Popelova O, Mokry M, Gersl V, Ponka P. J. Sep. Sci 2005;28:1300–1306. [PubMed: 16138682]
30. Kovarikova P, Mrkvickova Z, Klimes J. J. Pharm. Biomed. Anal 2008;47:360–370. [PubMed: 18294799]
31. Nakahara R, Fujimoto T, Doi M, Morita K, Yamaguchi T, Fujita Y. Chem. Pharm. Bull 2008;56:977–981. [PubMed: 18591813]

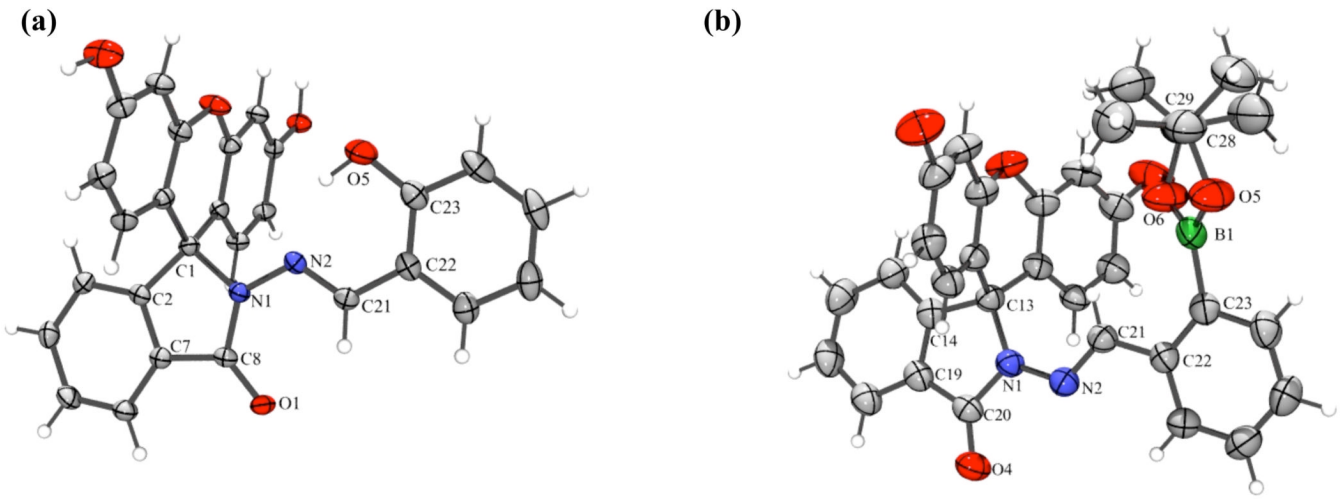

Fig. 1.

ORTEP structural diagrams showing 50% probability ellipsoids and partial atom numbering schemes for (a) FlamS and (b) FlamB (solvents of crystallization not shown). Select bond distances (Å) and angles (˚) for (a): C1–N1, 1.503(2); C8–N1, 1.364(2); N1–N2, 1.376(2); N2–C21, 1.285(2); C23–O5, 1.358(2); C1-N1-N2, 115.4(1); N1-N2-C21, 109.3(1); N2-C21-C22, 120.5(1); and (b): C13–N1, 1.490(3); C20– N1, 1.372(3); N1–N2, 1.373(3); N2–C21, 1.278(3); C23–B1, 1.547(4); B1–O5, 1.373(4); B1–O6, 1.348(4); N2-N1-C13, 127.8(2); N1-N2-C21, 118.9(2); N2-C21-C22, 119.7(2); O6-B1-O5, 113.0(3).

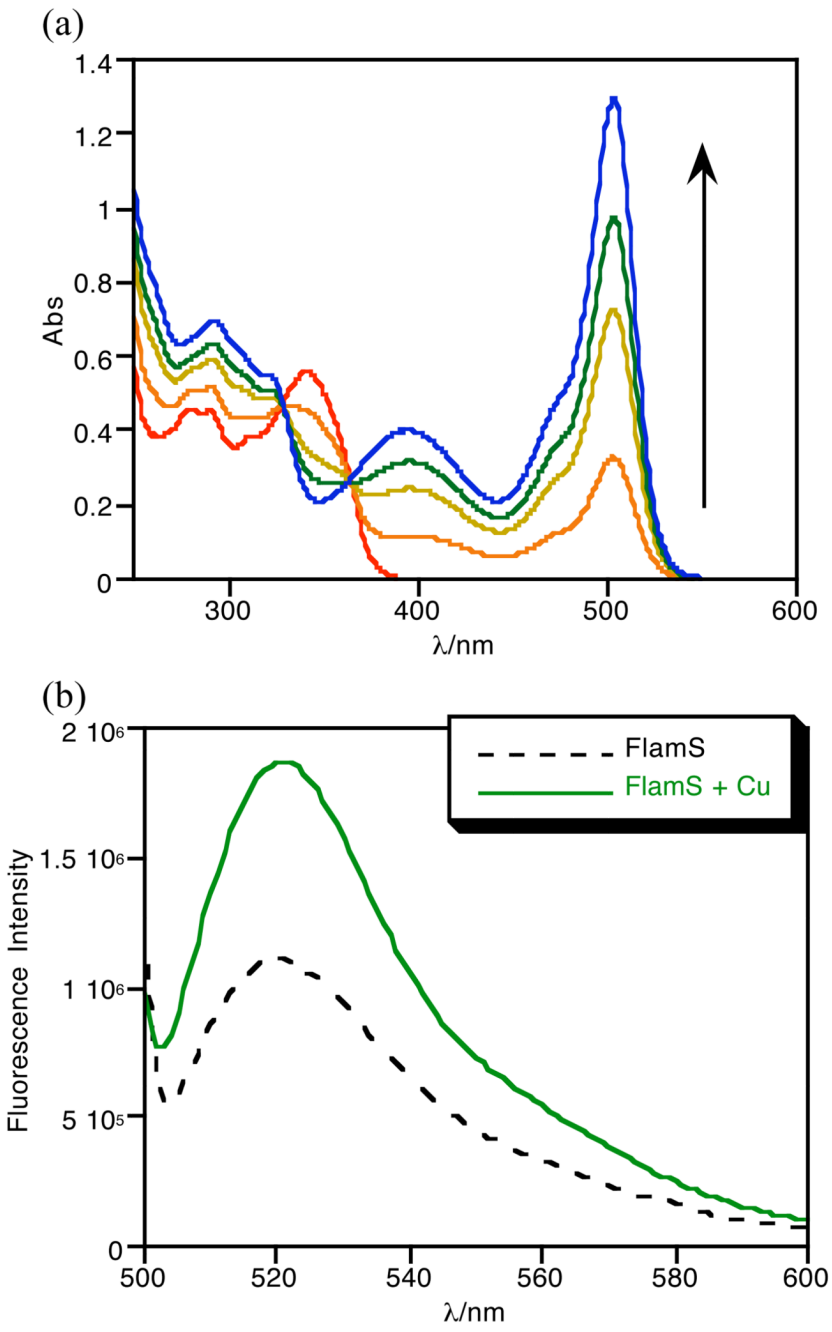

Fig. 2.

Absorbance spectra (a) of 40 μM FlamS in HEPES buffer (10 mM, pH = 7.4) containing 40% (v/v) DMSO titrated with $CuSO_4$ up to 1.25 eq. No further spectral changes are observed upon addition of excess Cu^{2+}. Emission spectra (b) of 10 μM FlamS in the same solvent conditions with 1 equivalent of $CuSO_4$. λ_{ex} = 495 nm.

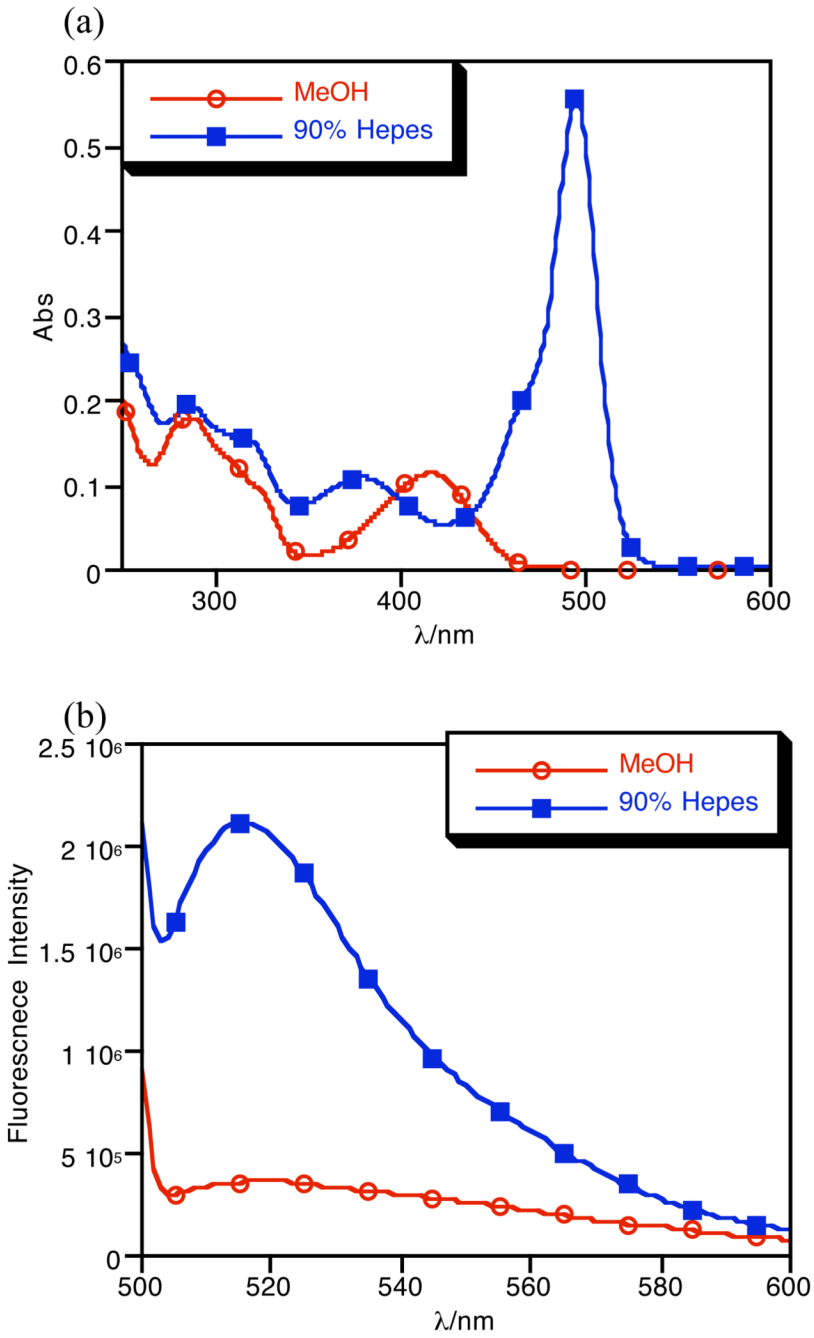

Fig. 3.

Absorbance (a) and emission (b) spectra of 10 μM $[Cu(FlamS)]^+$ in methanol and in HEPES buffer (10 mM, pH = 7.4) containing 10% (v/v) methanol. λ_{ex} = 495 nm.

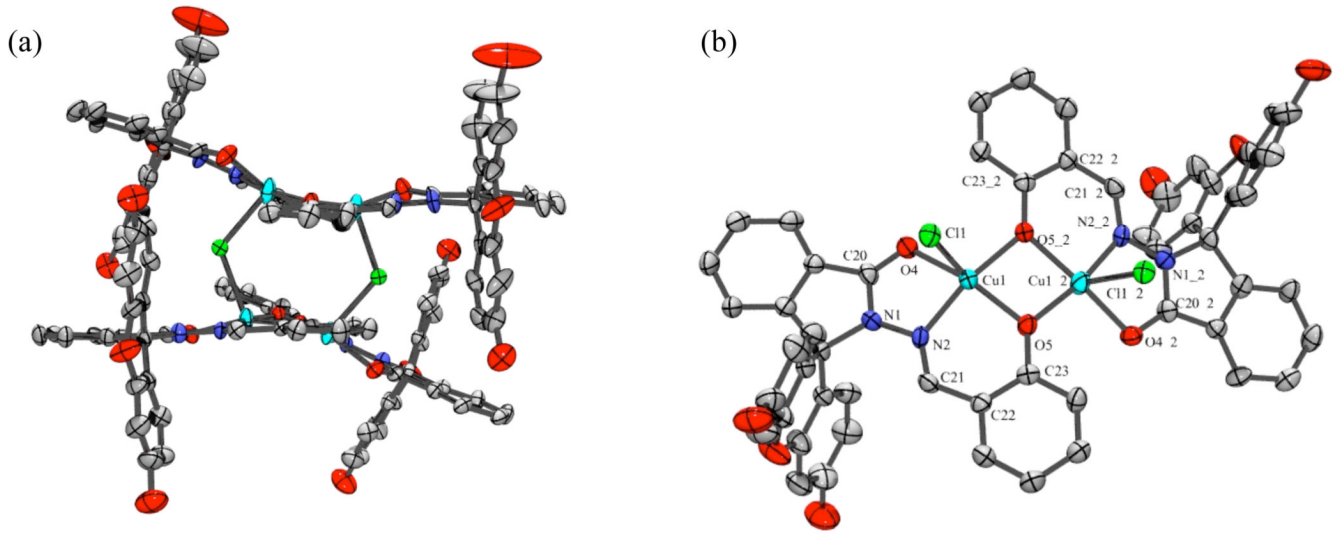

Fig. 4.

ORTEP structural diagram showing 50% probability ellipsoids and partial atom numbering schemes for Cu(II)-bound FlamS. (a) orientation showing the full tetranuclear arrangement of $[Cu_2Cl(FlamS)_2]_2^{2+}$ (two outer-sphere Cl^- anions not shown). (b) truncated orientation rotated forward 90° from (a) with two FlamS units deleted for clarity to highlight the coordination spheres around the Cu centers. The two units are related by a 2–fold rotation axis where the atoms labeled XX_2 are symmetry generated. Selected bond distances (Å) and angles (°): Cu1–O4, 2.041(4); Cu1–N2, 1.930(5); Cu1–O5, 1.943(4); Cu1–Cl1, 2.533(2); Cu1–O5_2, 1.913(4); N1–N2, 1.361(7); N2–C21, 1.291(8);

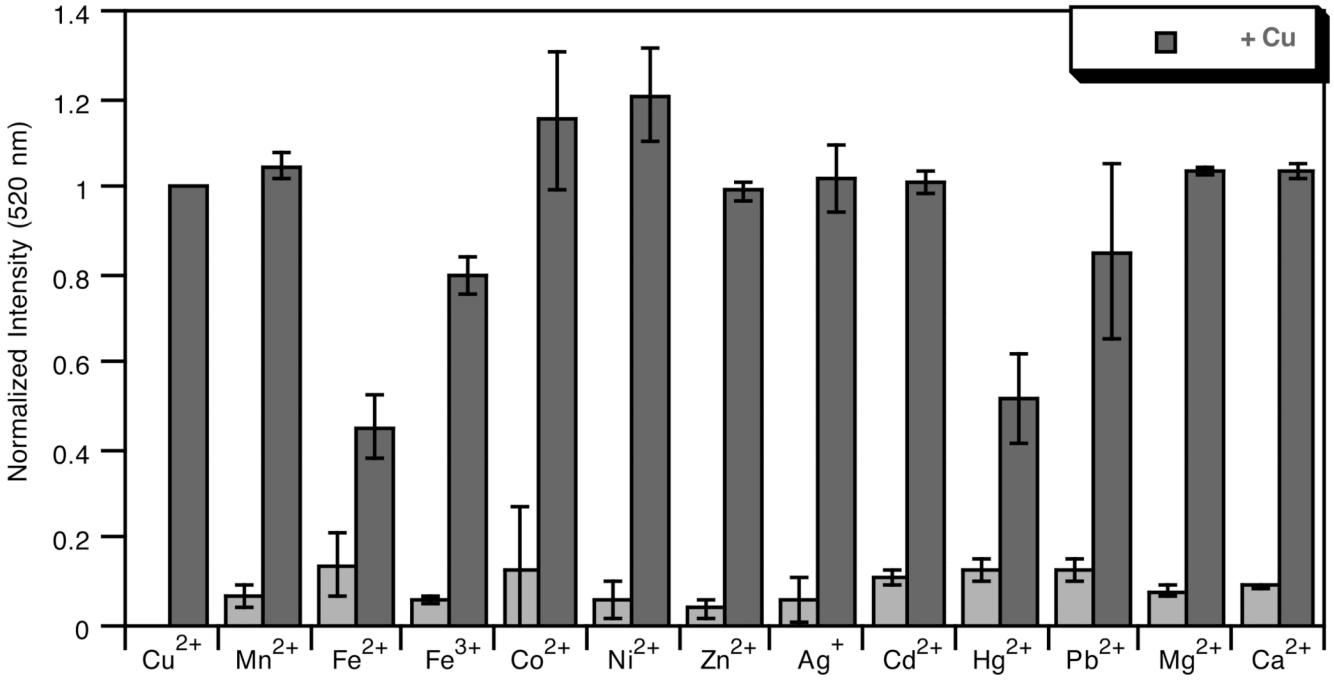

Fig. 5.

Light gray bars: Normalized fluorescence response at 520 nm of 10 μM solutions of FlamS to addition of various metal ions in HEPES buffer (10 mM, pH 7.4) containing 40% (v/v) DMSO. Metal stock solutions were prepared in H_2O from ferric ammonium citrate, $FeCl_2$, $NiCl_2$, $ZnCl_2$, $MnCl_2$, $CdSO_4$, $Hg(OAc)_2$, $Pb(NO_3)_2$, $CoCl_2$ and $AgNO_3$ and added to a final concentration of 20 μM, or 5 mM for $CaCl_2$ and $MgCl_2$. Dark gray bars: Fluorescence response after addition of 20 μM $CuSO_4$ to the FlamS–M^{n+} solutions. λ_{ex} = 495 nm.

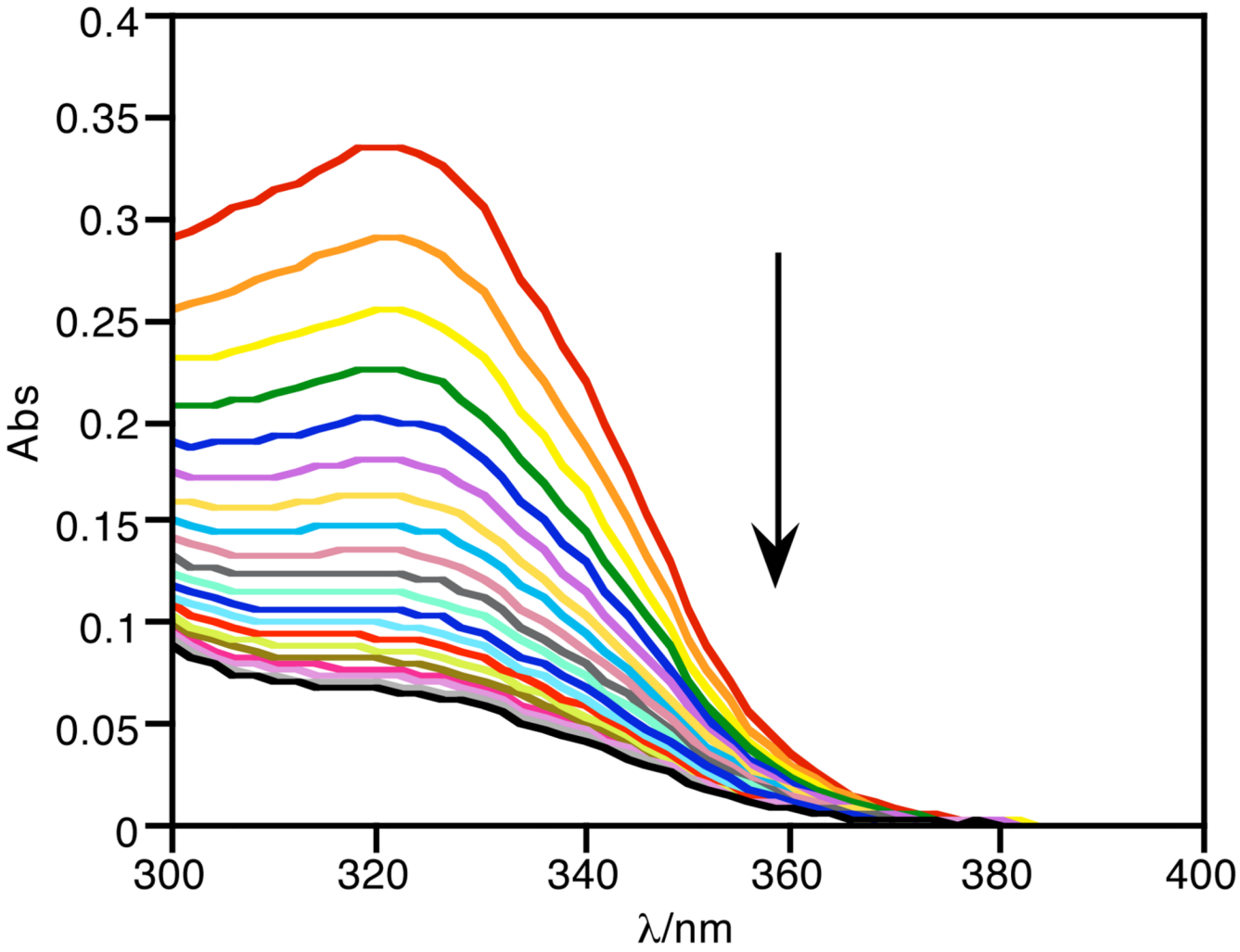

Fig. 6.

The decrease in absorbance at 325 nm of FlamB (20 μM) shows its instability in aqueous solution (HEPES buffer, 10 mM, pH = 7.4, containing 40% (v/v) DMSO). The spectra represent the first 30 min following dissolution.

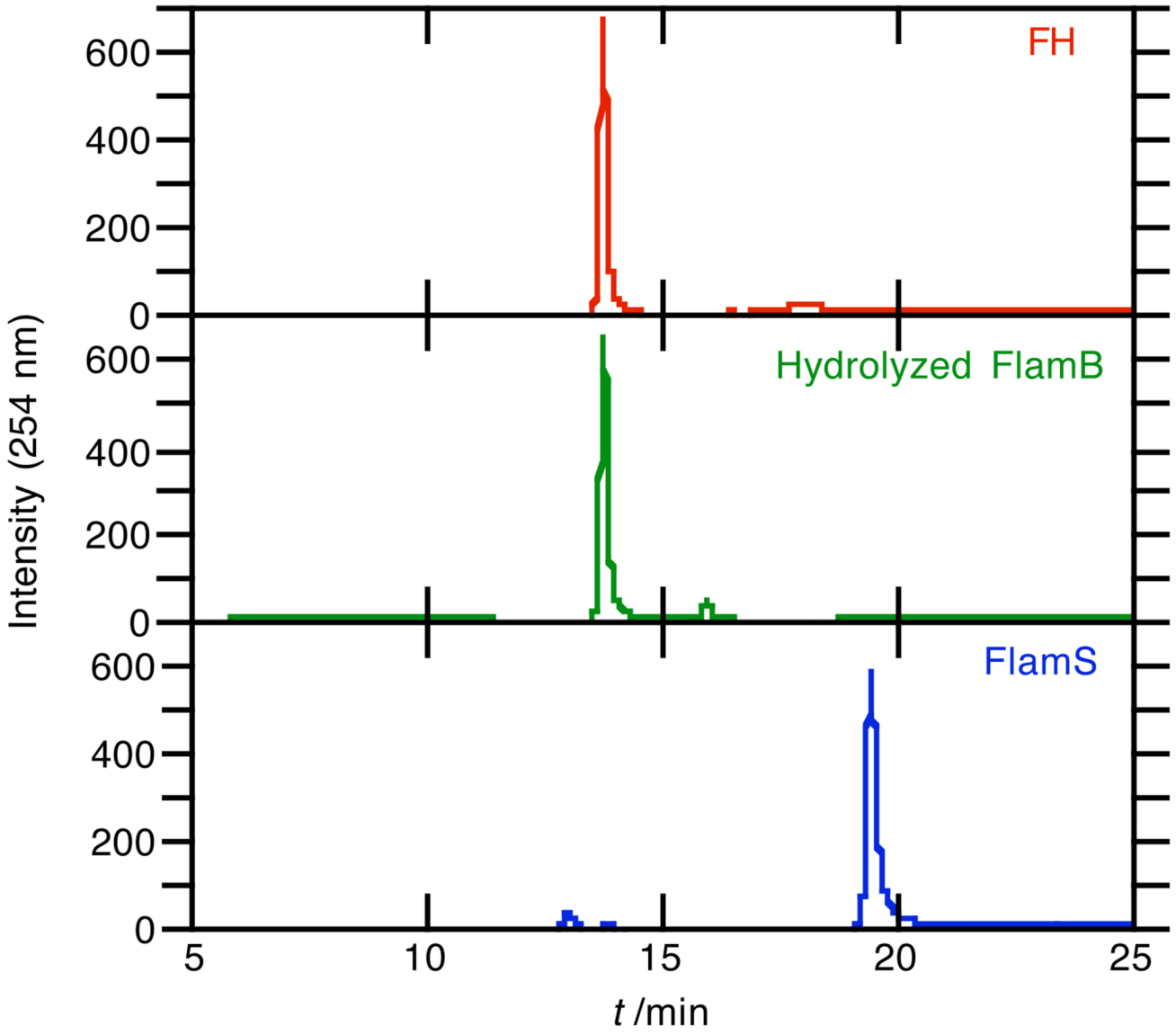

Fig. 7.

Chromatography traces for samples of 300 μM FH (top), FlamB (middle), and FlamS (bottom) that were analyzed 1.5 h after preparation in HEPES buffer (10 mM, pH = 7.4) containing 40% (v/v) DMSO. Mass spectra corresponding to the LC traces confirm the presence of FH in the FlamB sample, indicating that nearly all of the sample has hydrolyzed.

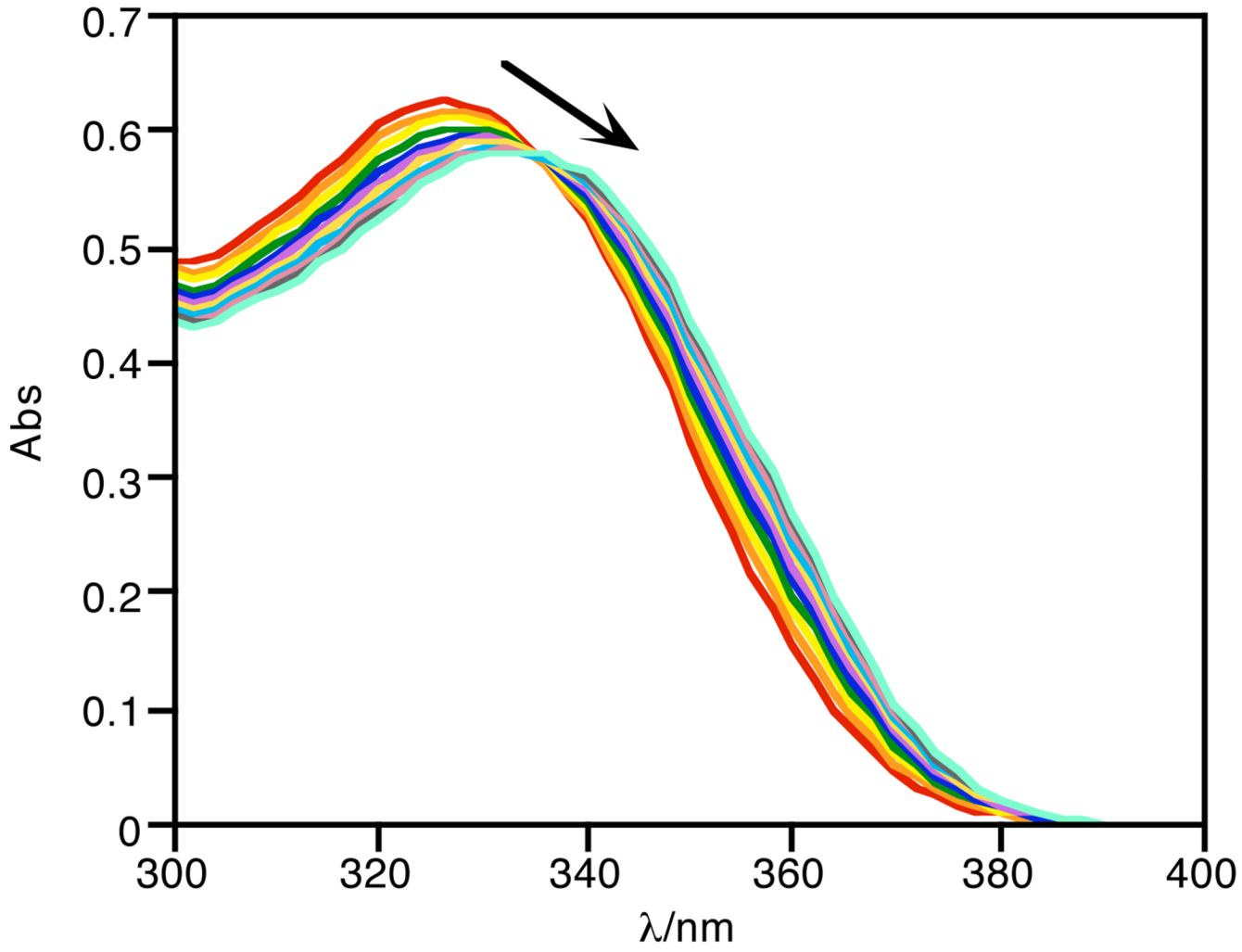

Fig. 8.
Conversion of FlamB (40 μM) to FlamS by oxidation with H_2O_2 (3 mM) in DMSO monitored for 2 h.

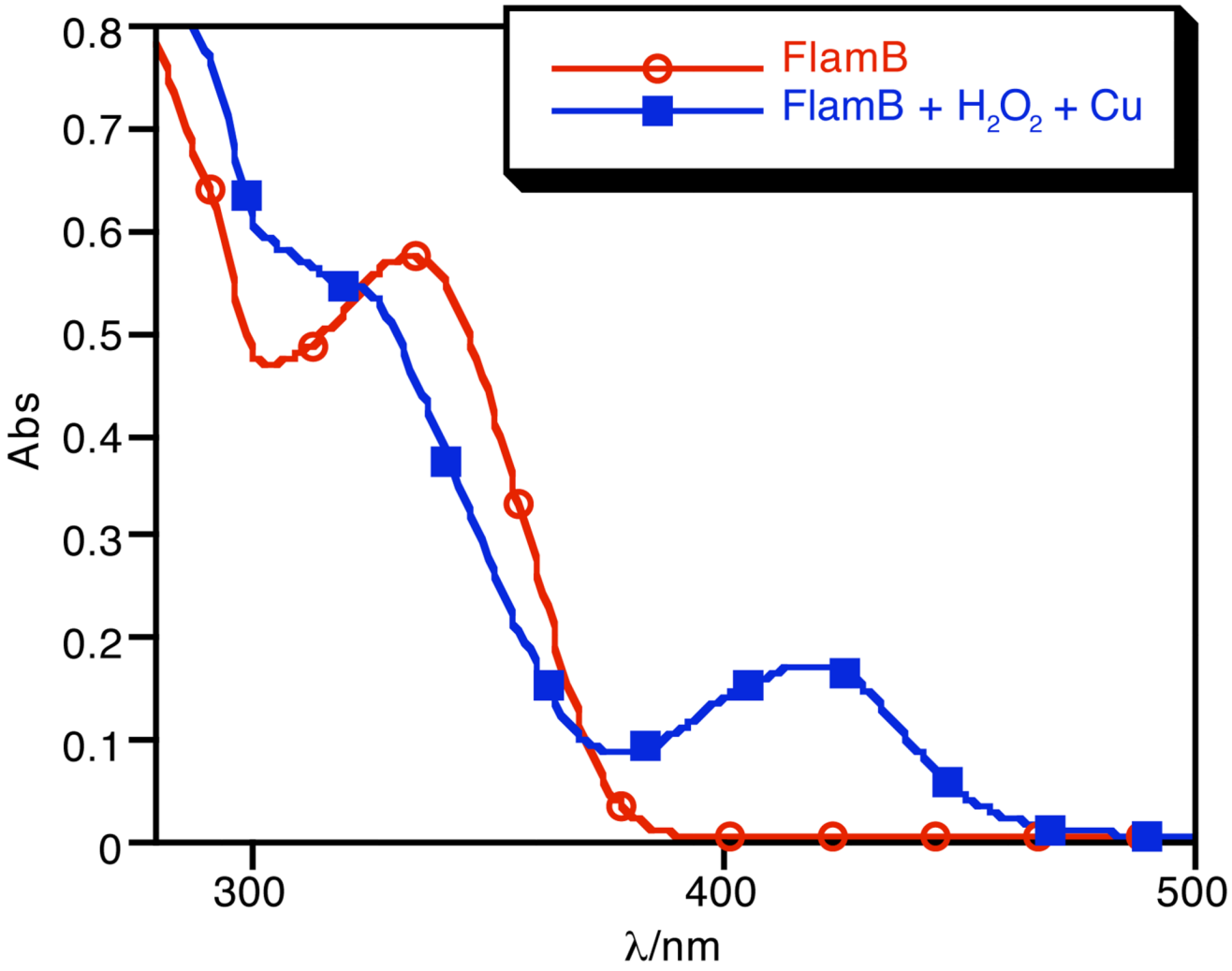

Fig. 9.
Addition of Cu^{2+} (40 μM) to a solution of FlamB (40 μM) oxidized with H_2O_2 (3 mM) for 2 h in DMSO.

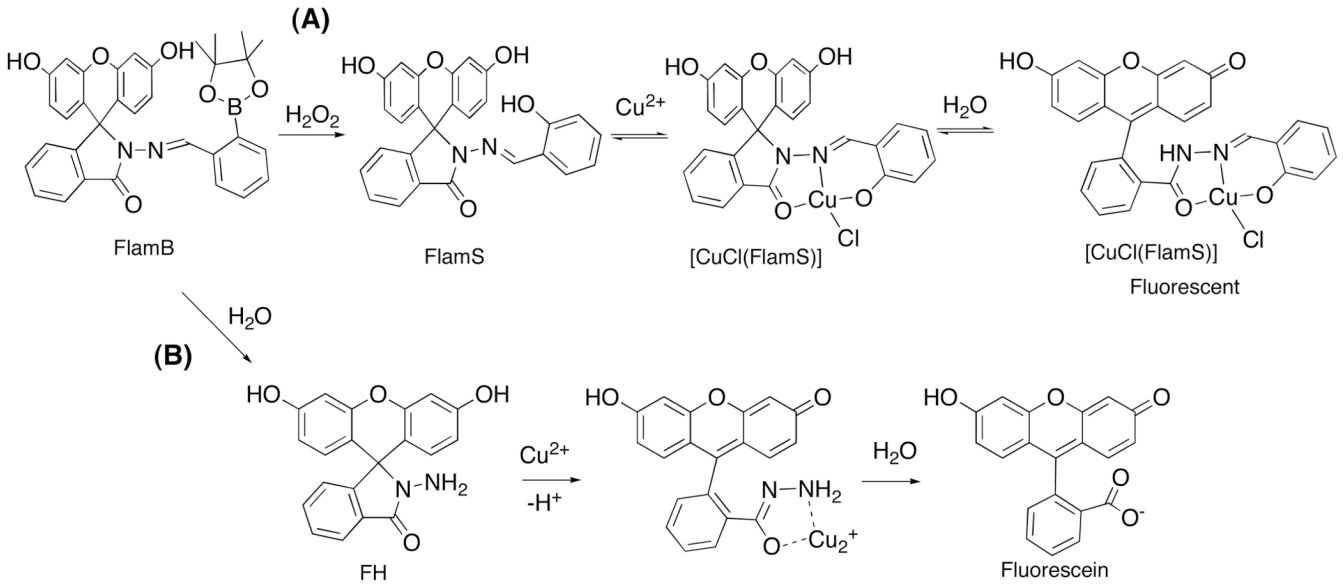

Scheme 1.

Alternate pathways to fluorescence enhancement. (A) FlamB oxidation followed by Cu^{2+} binding and spirolactam ring opening to give modestly fluorescent [CuCl(FlamS)] (drawn as the neutral monomer unit of the tetranuclear arrangement seen in the X-ray crystal structure), or (B) hydrolysis of FlamB to FH followed by reaction with Cu^{2+} to yield highly fluorescent fluorescein. FH also converts to fluorescein upon interaction with H_2O_2.[31]

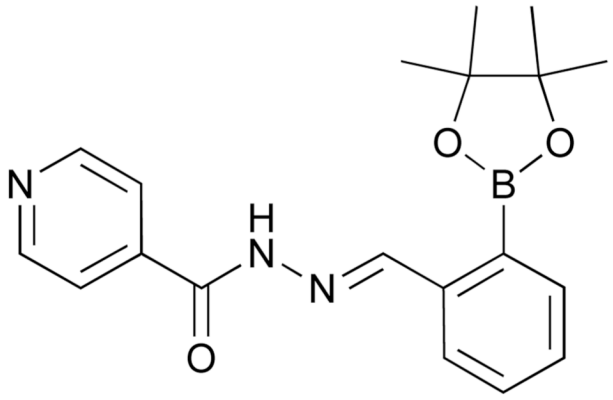

BSIH

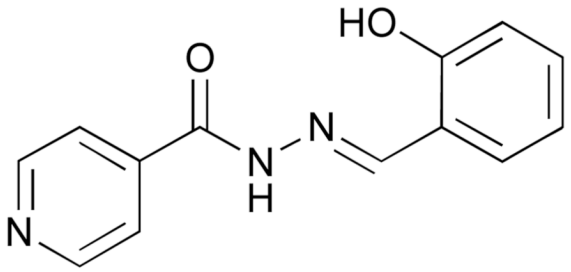

SIH

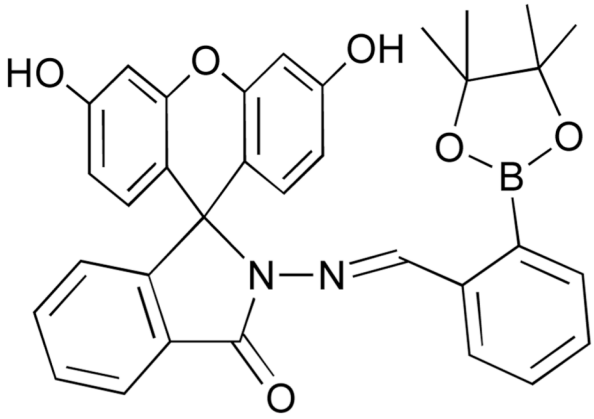

FlamB

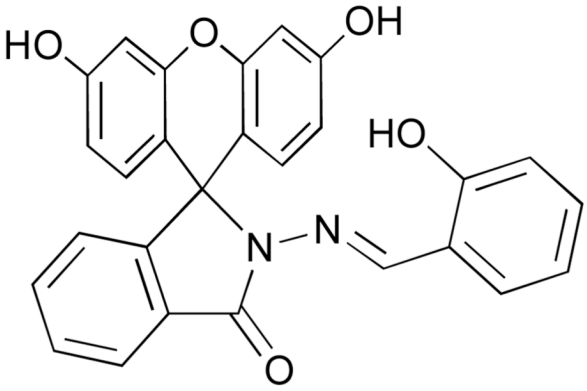

FlamS

Chart 1.